

## Electronic Structures of GaAs-AlAs(111) Superlattices and Interfaces

Eiichi YAMAGUCHI

*NTT Electrical Communications Laboratories*

*3-9-11 Midori-cho, Musashino-shi, Tokyo 180*

Electronic structures of GaAs-AlAs (111) superlattices are calculated using an extended version of the tight-binding method with an  $sp^3s^*$  basis. The results predict that the (111) superlattices exhibit features in the direct/indirect band crossover different from those of (001) or (110) superlattices. Specifically, in  $(\text{GaAs})_n(\text{AlAs})_n$  (111) superlattices, the  $\Gamma$  states are the lowest as far as  $n \geq 3$ . The calculated results further demonstrate that in (111) superlattices with imperfect interfaces, an "interface band" appears in the upper half of the bandgap. The implication of this result with respect to interpretation of experimental data is discussed.

### 1. Introduction

Recent developments in crystal growth technology have been successful in providing short period superlattices (SLs). Specifically, a GaAs-AlAs (001) SL has been extensively investigated both experimentally and theoretically. However, no report has ever been published on SLs with other interface orientations. In the present paper, the first theoretical results of electronic structures are demonstrated for GaAs-AlAs (111) SLs. The results are compared with those for the (001) and (110) SLs. The interface properties for the (111) SLs are also discussed.

### 2. Calculation

#### 2.1 Brillouin zone

Consider the  $(\text{GaAs})_n(\text{AlAs})_m$  (111) SLs with  $n + m = 3i$  ( $i = 1, 2, 3, \dots$ ). The Brillouin zone (BZ) for the (111) SLs with  $n + m = 3$  is shown in Fig. 1, where the corresponding fcc BZ is also shown with dotted lines. As shown in the figure, all X points of fcc BZ are folded into M points. This is an important fact for considering the effects of crystallographic orientation on the band structures of SLs. Namely, in the (001) and (110) SLs, the X points of fcc BZ are folded in different ways;  $X_z^c \equiv (0, 0, \pm 1)2\pi/a_L$  ( $a_L$  = lattice constant) go to  $\Gamma$ , and the other X points of fcc BZ,  $X_y$ , go to symmetry

points other than  $\Gamma$ . It is thus expected that the conduction band states at  $X_z$  and  $X_y$ , respectively, facilitate direct and indirect optical transitions in those SLs. The corresponding energies of these  $X_z^c$  and  $X_y^c$  states are expected to be different from each other. On the other hand, it is expected that in the (111) SLs, all the X states facilitate indirect transition with a single energy level.

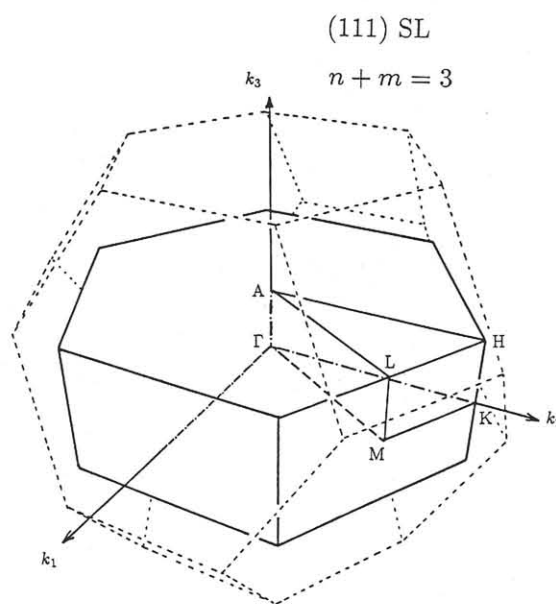


Fig. 1: Brillouin zone (BZ) for  $(\text{GaAs})_n(\text{AlAs})_m$  (111) SLs ( $n + m = 3$ ). Dotted lines represent BZ for the corresponding fcc.

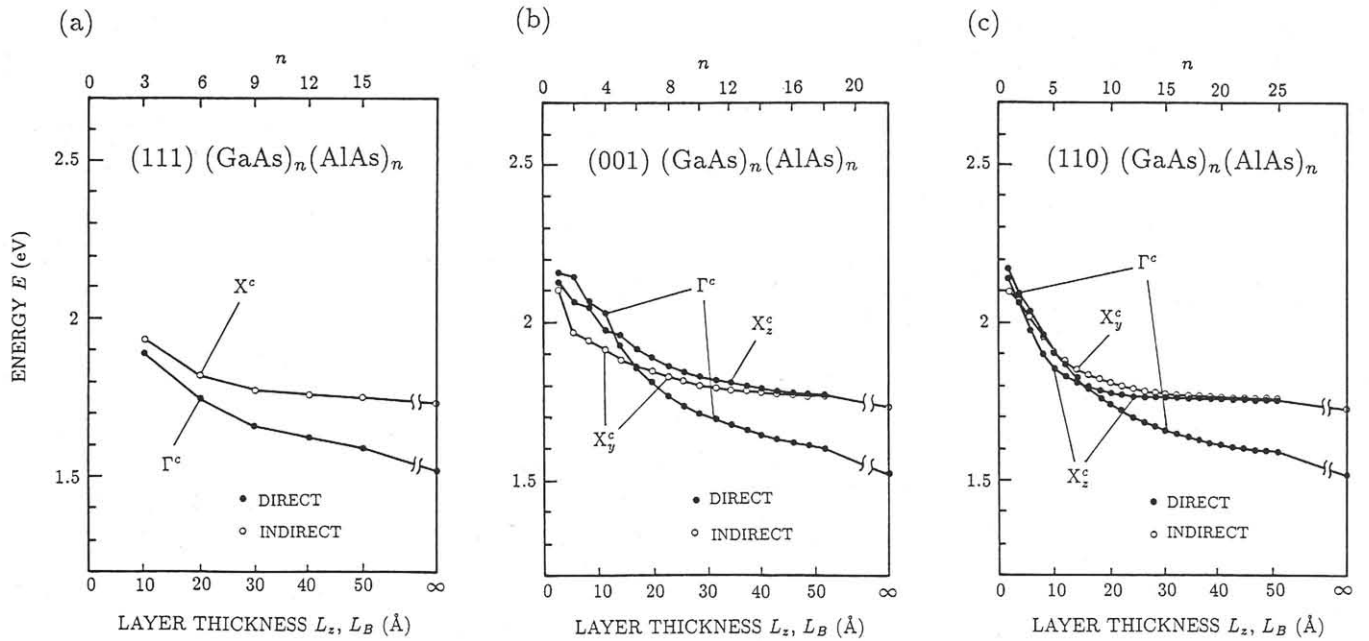


Fig. 2: Energies of conduction band minima at  $\Gamma$  and X as a function of layer thickness for (a) (111) SLs, (b) (001) SLs and (c) (110) SLs.

## 2.2 Tight-binding method

The  $sp^3s^*$  tight-binding method<sup>1)</sup> has been applied to  $(\text{GaAs})_n(\text{AlAs})_m$  (111) SL systems. The method and input parameters used here are the same as used in previous papers<sup>2,3)</sup>. A detailed description of the calculation method will be published elsewhere. The valence band offset is estimated to be 0.50 eV<sup>4)</sup>.

In GaAs-AlAs SLs, the bonds at the interface between GaAs and AlAs layers are in the direction perpendicular to the interface. The change in those intermaterial bond lengths,  $d_{\text{Ga-As}}$  and  $d_{\text{Al-As}}$ , will bring about a change in intermaterial interactions,  $\hat{H}_{\text{Ga-As}}$  and  $\hat{H}_{\text{Al-As}}$ . In the present work, these interactions are assumed to obey Harrison's  $d^{-2}$  scaling law<sup>5)</sup>;  $\hat{H}_{\text{Ga-As}} \propto d_{\text{Ga-As}}^{-2}$  and  $\hat{H}_{\text{Al-As}} \propto d_{\text{Al-As}}^{-2}$ . Thus, the effect of interface imperfectness on the electronic structures has been investigated by changing the parameters  $d_{\text{Ga-As}}/d_0$  and  $d_{\text{Al-As}}/d_0$ , where  $d_0$  is the bond length for the perfect crystal.

## 3. Results and Discussion

### 3.1 Bandgap

In Fig. 2(a), the calculated energies of the conduction band minima at the  $\Gamma$ -points ( $\Gamma^c$ ) and X-

points ( $X^c$ ) for  $(\text{GaAs})_n(\text{AlAs})_n$  (111) SLs are shown as a function of GaAs thickness  $L_z$  ( $=\text{AlAs}$  thickness  $L_B$ ) or the period  $n$ . Here, the energies are measured from the valence band maximum. For comparison, the results for  $(\text{GaAs})_n(\text{AlAs})_n$  (001) and (110) SLs are shown in Figs. 2(b) and 2(c). As seen from these figures, the  $\Gamma^c$  state is the lowest as far as  $n \geq 3$  in the (111) SLs. On the other hand, in the (001) SLs, the  $X_y^c$  states (indirect) are lower than the  $X_z^c$  states (direct) for small  $n$ , and become the lowest when  $n$  becomes smaller than 6<sup>3)</sup>.

Contrary to the case in the (001) SLs, the  $X_z^c$  states (direct) are lower than the  $X_y^c$  states (indirect) in the (110) SLs with  $n > 1$ . The  $X_z^c$  states become the lowest when  $n$  becomes smaller than 7. When  $n$  is equal to 1, the system is equivalent to the (001) SL, and the  $X_y^c$  states become the lowest. Therefore, it can be predicted that (110) SLs with  $n > 1$  will exhibit a direct transition. However, the transition probability will strongly decrease when  $n$  becomes smaller than 7. This is because the conduction band states,  $X_z^c$ , are more or less localized in AlAs layers<sup>3)</sup>.

In Fig. 3, the characteristics of the conduction band states are shown as a function of GaAs ( $L_z$ ) and AlAs ( $L_B$ ) thickness for the (a)(111), (b)(001)

and (c)(110) SLs. As shown in Fig. 3(a) and 3(b), there is a region in which the (111) SLs exhibit a strong direct transition but the (001) SLs are incapable of this transition<sup>6</sup>). Thus, it can be concluded that short period GaAs-AlAs (111) SLs will provide materials applicable to optical devices with higher photoluminescence energies than the (001) SLs.

It is also shown in Fig. 3(c) that the (110) SLs with  $L_z < 5 \text{ \AA}$  and  $L_B > 10 \text{ \AA}$  has potential importance for application to high energy optical devices. This is because the conduction band states,  $X_z^c$ , which facilitate a direct transition are only minimally confined to the AlAs layers when  $L_z$  becomes smaller than about  $5 \text{ \AA}$ .

### 3.2 Interface band

The band structure for the  $(\text{GaAs})_{15}(\text{AlAs})_{15}$  (111) SL with perfect and imperfect ( $d_{\text{Ga-As}}/d_0 = 2$ ) interfaces are, respectively, shown in Fig. 4(a) and 4(b). As clearly seen from these figures, "interface bands" appear in the bandgap in the SLs with imperfect interfaces. Especially, the interface band which gives the lowest conduction band forms valleys with extremely heavy mass around the M points. The corresponding wave functions are found to be strongly localized at the interfaces.

The band structure for the GaAs-ZnSe SL with imperfect interfaces has also been calculated in order to show that these interface band features depend only on the electronic characters of GaAs, whenever the material with which GaAs forms a heterostructure has a higher conduction band minimum than GaAs. The result for  $(\text{GaAs})_{15}(\text{ZnSe})_{15}$  (111) SLs with  $d_{\text{Ga-Se}}/d_0 = 2$  is shown in Fig. 4(c). Here, the valence band offset is estimated to be  $0.96 \text{ eV}$ <sup>7</sup>). It is shown in this figure that the same type of interface band as in the GaAs-AlAs SLs are induced in the upper half of the bandgap when the interface imperfectness is introduced. Therefore it can be concluded that the present interface band characteristics result from the GaAs band characters.

This interface band results in a large density of states in the bandgap, as shown in Fig. 5. It has further been found that the interface band appears whenever  $d_{\text{inter}}/d_0$  is larger than 1.2. When  $d_{\text{inter}}/d_0$

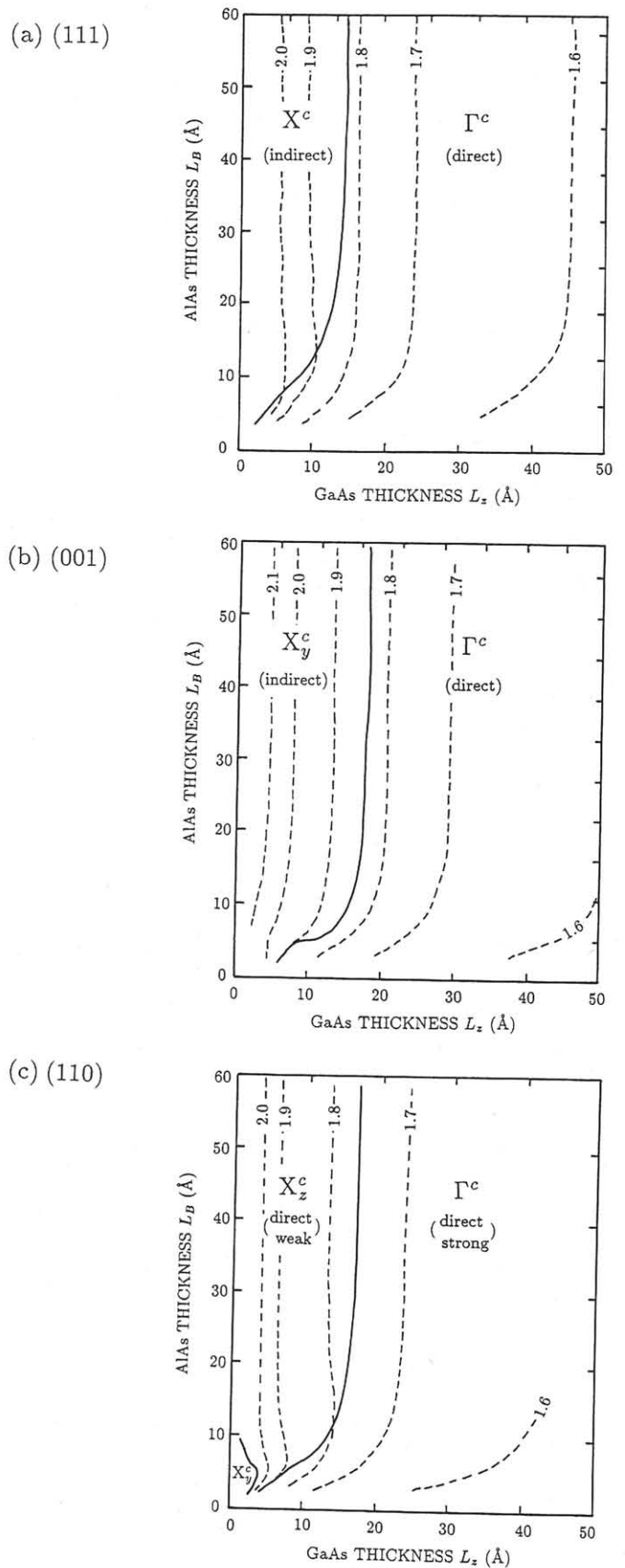


Fig. 3: Conduction band characters for (a)(111) SLs, (b)(001) SLs and (c)(110) SLs. Dashed lines represent the contour lines for the bandgap in units of eV.

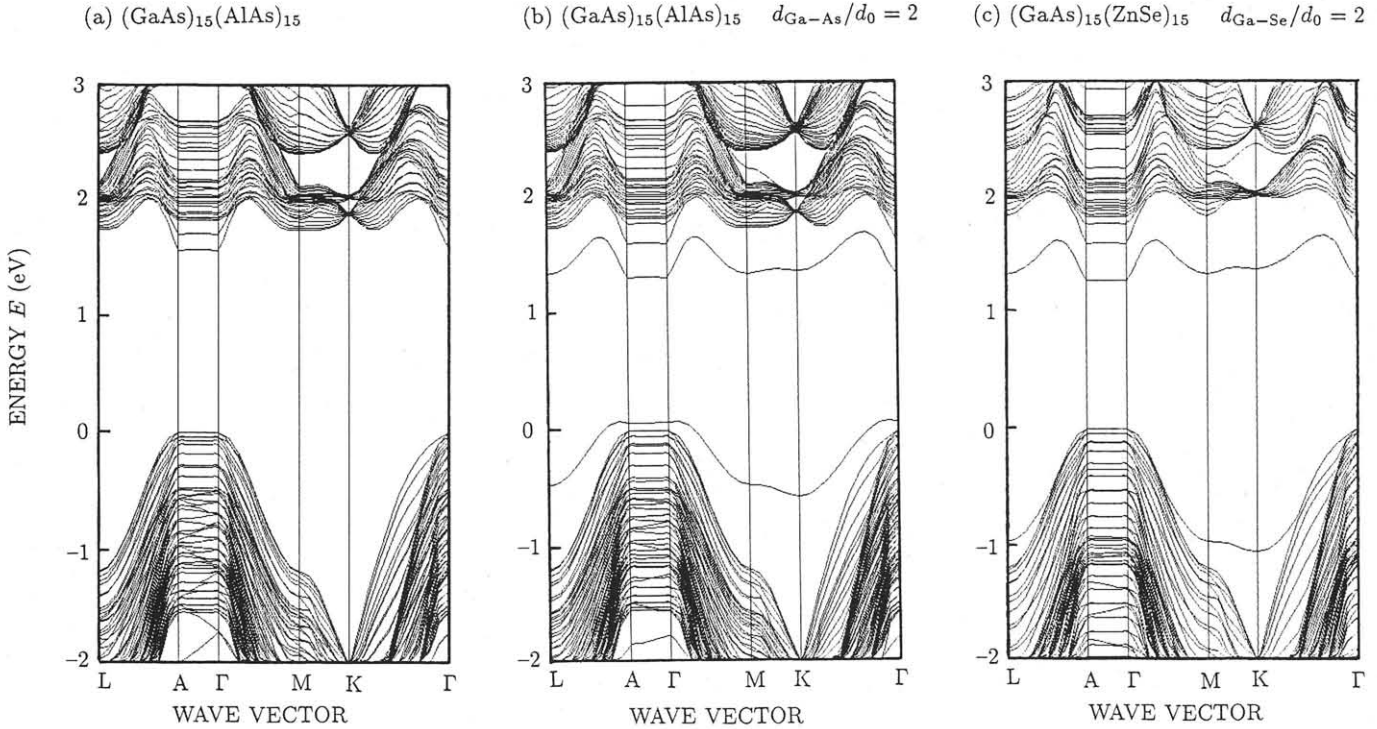


Fig. 4: Band structures for (a) perfect  $(\text{GaAs})_{15}(\text{AlAs})_{15}$  SL, (b)  $(\text{GaAs})_{15}(\text{AlAs})_{15}$  SL ( $d_{\text{Ga-As}}/d_0 = 2$ ) and (c)  $(\text{GaAs})_{15}(\text{ZnSe})_{15}$  SL ( $d_{\text{Ga-Se}}/d_0 = 2$ ).

increases, the valleys around M points are slightly lowered and then almost fixed in the upper half of the bandgap. This feature is very similar to the gap states characters of GaAs/insulator interfaces. The present results can therefore provide a novel model for the origin of the interface states in GaAs MIS systems.

#### Acknowledgment

The author greatly appreciates the fruitful discussions of Yoshitaka Furukawa, Osamu Mikami, Mitsuru Naganuma, Hidetoshi Iwamura, Yoshifumi Suzuki, Takahisa Ohno and Masami Kumagai.

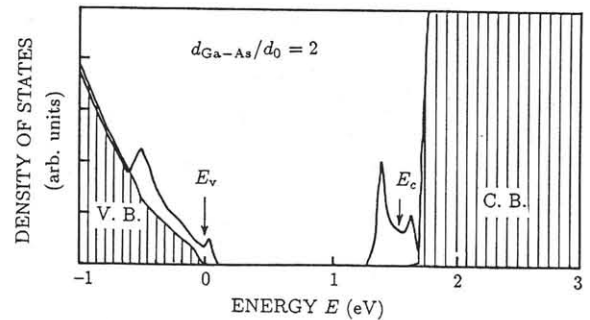


Fig. 5:

Density of states for  $(\text{GaAs})_{15}(\text{AlAs})_{15}$  SL ( $d_{\text{Ga-As}}/d_0 = 2$ ). Shaded area represents the density of states for perfect  $(\text{GaAs})_{15}(\text{AlAs})_{15}$  SL.

#### References

- 1) P. Vogl, H. P. Hjalmarson and J. D. Dow, *J. Phys. Chem. Solids* **44**, 365(1983).
- 2) E. Yamaguchi, Tech. Rep. Inst. Electron. & Commun. Eng. Jpn. **ED86-55**, 43(1986) [in Japanese].
- 3) E. Yamaguchi, *J. Phys. Soc. Jpn.* **56**, No.8(1987) [in press].
- 4) H. Kroemer, *Conf. Workbook of the 2nd Int. Conf. on Modulated Semiconductor Structures*, Sept. 9-13, Kyoto, 1985, p.797.
- 5) W. A. Harrison, *Electronic Structure and Properties of Solids* (Freeman, San Francisco, 1980).
- 6) Very recently, Ihm has independently obtained a similar result for the (001) SLs. [*Appl. Phys. Lett.* **50**, 1068(1987)].
- 7) S. P. Kowalczyk, E. A. Kraut, J. R. Waldrop and R. W. Grant, *J. Vac. Sci. Technol.* **21**, 482(1982).